www.rericjournal.ait.ac.th

Fuzzy Logic Based Load Frequency Control of Multi-Area Electrical Power System Considering Non-Linearities and Boiler Dynamics

Yogendra Arya*[1], Narendra Kumar[+], and S.K. Sinha[#]

Abstract – *This paper presents the Load Frequency Control (LFC) of four-area interconnected reheat thermal power system using fuzzy logic based PI controller (FLPI). The system is incorporated with governor dead band, generation rate constraint non-linearities and boiler dynamics. The conventional PI controller does not yield adequate control performance when considering the non-linearities and boiler dynamics. The aim of FLPI controller is to restore the frequency and tie-line power very smoothly to its nominal value in the shortest possible time. Four performance criteria i.e. settling time, peak overshoot, integral absolute error (IAE) and integral of time multiplied absolute error (ITAE) are utilized for the comparison. The comparison between the conventional PI controller and the proposed controller show that the proposed controller can generate the best dynamic response following a load perturbation. Robustness of the proposed controller is achieved by analyzing the system responses with varying system parameters.*

Keywords – Area control error, boiler dynamics, fuzzy logic controller, generation rate constraint, governor deadband.

1. INTRODUCTION

The main objectives of an interconnected electrical power system control are generating, transmitting, and distributing electric power as economically and reliably as possible while maintaining the quality of power, voltage magnitude, and frequency within the acceptable limits. Large-scale power systems comprise interconnected subsystems (control areas) forming coherent groups of generators, whereas connection between the areas is made using tie-lines. Each control area has its own generation and is responsible for its own load and scheduled interchanges with neighbouring areas. The load in a given power system is continuously changing, consequently the system frequency and tie-line flows deviate from the nominal values. The load frequency controller is needed to maintain the system frequency and inter-area flows at the desired nominal values. Steam input to turbo generators (or water input to hydro generators) must continuously be regulated to match the active power demand, failing which the machine speed will vary with consequent change in frequency, which may be highly undesirable as frequency variations in interconnected power systems can cause large-scale serious instability problems [1]. Since frequency of power system is mainly affected by change in active power and voltage magnitude is mainly affected by change in reactive power, these are controlled separately [2]-[3]. Two control loops *i.e.* primary frequency control loop and secondary frequency loops, are used to achieve load frequency control (LFC). The main function of the LFC is to eliminate the frequency and net tie-line interchange deviations [4]. In multi-area power system, if a load variation occurs at any one of the areas in the system, the frequency related with this area is affected first and then that of other areas are also affected from this perturbation through tie-lines. Therefore, a control strategy is needed, that not only maintains constancy of frequency and desired tie-power flow but also achieves zero steady state error and inadvertent interchange.

Several control strategies, such as optimal control [2], [5], suboptimal control [6]-[8], classical control [9]-[10], adaptive control [11]-[13] *etc.* have been employed in the past to explore an optimum controller for LFC. The conventional control strategy for LFC problem is to take the integral of area control error (ACE) as the control signal. LFC systems basically use simple integral controller and PI controller, whose parameters are usually tuned based on classical control or trial-error approaches. The integral controller provides zero steady-state frequency deviation but it exhibits poor dynamic performance. The basic approaches to design controllers are not effective to obtain good dynamic performance for various load changes scenarios and disturbances in an interconnected power system. Adaptive controllers with self-adjusting gain settings have been proposed to overcome this deficiency. Despite the promising results achieved by these adaptive controllers, the control adjustments are complicated and require online system model identification. Centralized information structure and knowledge of all system parameters are technically difficult and economically unjustifiable. There are some authors who have applied variable structure control [14]-[17] to make the controller insensitive to system parameters change. Artificial neural networks have been successfully applied to the LFC problem with the promising results [18]-[22]. Moreover fuzzy logic control techniques [23]-[28] for LFC problem are mostly based on fuzzy gain scheduling of integral and proportional integral (PI) controller parameters. A hybrid neuro fuzzy control strategy has been proposed

*Department of Electrical and Electronics Engineering, Maharaja Surajmal Institute of Technology, New Delhi-110058, India.

[+]Department of Electrical Engineering, Delhi Technological University, Shahbad Daulatpur, Delhi-110042, India.

[#]Department of Electrical Engineering, Galgotias University, Greater Noida-201308, India.

[1]Corresponding author; Tel: + 919891484801.
E-mail: y_arya40@yahoo.com.

for LFC to improve performance of the fuzzy controller in [29]-[30]. Many researchers have applied genetic algorithm (GA) controllers to improve the dynamic performance of the power system [31]-[33].

In most of the research papers the various non-linarites *e.g.* generation rate constraints (GRC), the governor deadband (GDB), and the boiler dynamics (BD) effects have been neglected in the load frequency control studies for simplicity. But for the realistic analysis of system performance, it shall be adequate to incorporate these effects. As per literature researchers [34]-[39] used these effects for load frequency control in power systems but in all works investigations are limited to two-area system only. Ngamroo [40] used three-area thermal power system for his study. Now in present study, LFC of four-area single reheat thermal power system with GRC, GDB, and BD is presented by using PI/FLPI controllers. The main investigations of the present work are:

a) To design conventional proportional integral (PI) and the fuzzy logic based proportional integral (FLPI) controllers and to apply the same in four-area reheat thermal power system equipped with equal and unequal power ratings.
b) To compare the dynamic performance of fuzzy logic based proportional integral (FLPI) and conventional PI controllers at different load disturbances.
c) To test the robustness of the FLPI controller for wide change in parameters of the system under study.

2. FOUR-AREA POWER SYSTEM

Investigations have been carried out first on a four-area reheat thermal power system with equal power ratings (each area of 2000MW), then a four-area reheat thermal power system with unequal power ratings (area 1: 2000MW, area 2: 4000MW, area 3: 6000MW, and area 4: 8000MW) have been investigated. Thermal areas are provided with single reheat thermal turbine in each area. An interconnected power system is considered as being divided into control areas, connected by tie-lines. In each control area, all generators are assumed to form a coherent group. The power system investigated is interconnected by six tie lines as shown in Figures 1 and 2. For conventional integral controller the overall system given in Figures 2 and 3 can be model in a state space form of:

$$\dot{x} = A\,x + B\,u + F\,w \qquad (1)$$

where,

$x = [x_1 \quad x_2 \quad \bullet \quad \bullet \quad \bullet \quad x_{22}]^T$ = state vector,

$u = [u_1 \quad u_2 \quad u_3 \quad u_4]^T$ = control vector,

$\Delta P_d = w = [w_1 \quad w_2 \quad w_3 \quad w_4]^T$ = disturbance vector,

A is system matrix, B, and F are the input and disturbance distribution matrices respectively. Let,

$x_1 = \Delta f_1 \quad x_2 = \Delta P_{g1} \quad x_3 = \Delta y_{E1}$

$x_4 = \Delta f_2 \quad x_5 = \Delta P_{g2} \quad x_6 = \Delta y_{E2}$

$x_7 = \Delta f_3 \quad x_8 = \Delta P_{g3} \quad x_9 = \Delta y_{E3}$

$x_{10} = \Delta f_4 \quad x_{11} = \Delta P_{g4} \quad x_{12} = \Delta y_{E4}$

$x_{13} = \Delta P_{tie,\,12}$

$x_{14} = \Delta P_{tie,\,31}$

$x_{15} = \Delta P_{tie,\,41}$

$x_{16} = \Delta P_{tie,\,34}$

$x_{17} = \Delta P_{tie,\,32}$

$x_{18} = \Delta P_{tie,\,42}$

$x_{19} = \int ACE_1 dt \quad w_1 = \Delta P_{d1}$

$x_{20} = \int ACE_2 dt \quad w_2 = \Delta P_{d2}$

$x_{21} = \int ACE_3 dt \quad w_3 = \Delta P_{d3}$

$x_{22} = \int ACE_4 dt \quad w_4 = \Delta P_{d4}$

So the matrices B and F are given as:

$$B^T = \begin{bmatrix} 0 & 0 & \frac{1}{T_{sg1}} & 0 & 0 & 0 & 0 & 0 & 0 & 0 & 0 & 0 & 0 & 0 & 0 & 0 & 0 & 0 & 0 & 0 & 0 & 0 \\ 0 & 0 & 0 & 0 & 0 & \frac{1}{T_{sg2}} & 0 & 0 & 0 & 0 & 0 & 0 & 0 & 0 & 0 & 0 & 0 & 0 & 0 & 0 & 0 & 0 \\ 0 & 0 & 0 & 0 & 0 & 0 & 0 & 0 & \frac{1}{T_{sg3}} & 0 & 0 & 0 & 0 & 0 & 0 & 0 & 0 & 0 & 0 & 0 & 0 & 0 \\ 0 & 0 & 0 & 0 & 0 & 0 & 0 & 0 & 0 & 0 & 0 & \frac{1}{T_{sg4}} & 0 & 0 & 0 & 0 & 0 & 0 & 0 & 0 & 0 & 0 \end{bmatrix}$$

$$F^T = \begin{bmatrix} -\frac{K_{ps1}}{T_{ps1}} & 0 & 0 & 0 & 0 & 0 & 0 & 0 & 0 & 0 & 0 & 0 & 0 & 0 & 0 & 0 & 0 & 0 & 0 & 0 & 0 & 0 \\ 0 & 0 & 0 & -\frac{K_{ps2}}{T_{ps2}} & 0 & 0 & 0 & 0 & 0 & 0 & 0 & 0 & 0 & 0 & 0 & 0 & 0 & 0 & 0 & 0 & 0 & 0 \\ 0 & 0 & 0 & 0 & 0 & 0 & -\frac{K_{ps3}}{T_{ps3}} & 0 & 0 & 0 & 0 & 0 & 0 & 0 & 0 & 0 & 0 & 0 & 0 & 0 & 0 & 0 \\ 0 & 0 & 0 & 0 & 0 & 0 & 0 & 0 & -\frac{K_{ps4}}{T_{ps4}} & 0 & 0 & 0 & 0 & 0 & 0 & 0 & 0 & 0 & 0 & 0 & 0 & 0 \end{bmatrix}$$

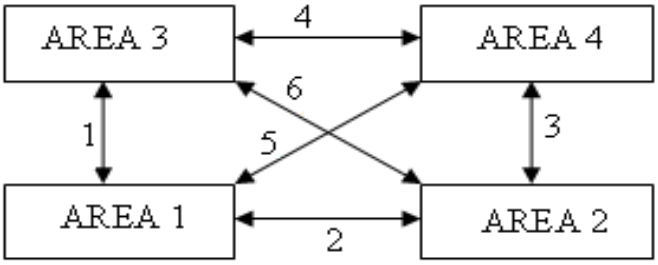

Fig. 1. Schematic diagram of interconnected four-area power system with six tie lines.

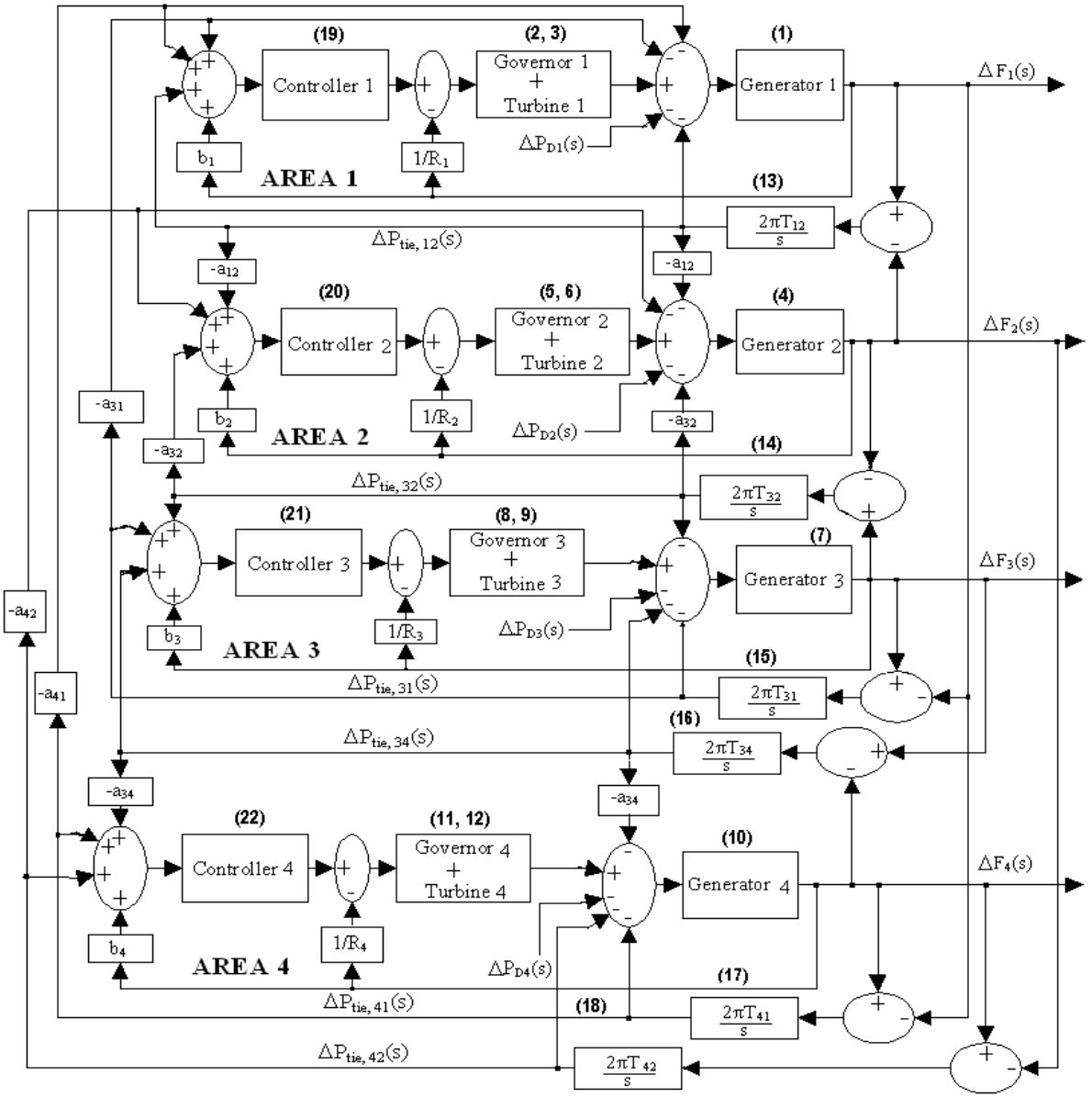

Fig. 2. Block diagram of four-area interconnected power system.

The control signals u_1, u_2, u_3, and u_4 for the speed changers of the four-area power system will be given as:

$$u_1 = -k_{i1} x_{19} = -k_{i1} \int ACE_1 dt = \Delta P_{C1}(s)$$
$$u_2 = -k_{i2} x_{20} = -k_{i2} \int ACE_2 dt = \Delta P_{C2}(s) \quad (2)$$
$$u_3 = -k_{i3} x_{21} = -k_{i3} \int ACE_3 dt = \Delta P_{C3}(s)$$
$$u_4 = -k_{i4} x_{22} = -k_{i4} \int ACE_4 dt = \Delta P_{C4}(s)$$

$$x_{19} = \int ACE_1 dt, \quad x_{20} = \int ACE_2 dt$$
$$x_{21} = \int ACE_3 dt, \quad x_{22} = \int ACE_4 dt \quad (3)$$

where,

$$ACE_1 = \Delta P_{tie,12} + \Delta P_{tie,13} + \Delta P_{tie,14} + b_1 \Delta f_1$$
$$ACE_2 = \Delta P_{tie,21} + \Delta P_{tie,23} + \Delta P_{tie,24} + b_2 \Delta f_2$$
$$ACE_3 = \Delta P_{tie,31} + \Delta P_{tie,32} + \Delta P_{tie,34} + b_3 \Delta f_3$$
$$ACE_4 = \Delta P_{tie,41} + \Delta P_{tie,42} + \Delta P_{tie,43} + b_4 \Delta f_4$$

K_{ii} is integral gain, ACE_i is the area control error and ΔP_{ci} is the change in speed changer setting of the ith area. Using Equation 2 and Equation 3, B merges in A and Equation 1 turns to

$$\dot{x} = A x + F w \quad (4)$$

where, A is given as:

$$A=\begin{bmatrix}
-\frac{1}{T_{ps1}} & \frac{K_{ps1}}{T_{ps1}} & 0 & 0 & 0 & 0 & 0 & 0 & 0 & 0 & 0 & 0 & -\frac{K_{ps1}}{T_{ps1}} & \frac{a_{31}K_{ps1}}{T_{ps1}} & \frac{a_{41}K_{ps1}}{T_{ps1}} & 0 & 0 & 0 & 0 & 0 & 0 & 0\\
0 & -\frac{1}{T_{t1}} & \frac{1}{T_{t1}} & 0 & 0 & 0 & 0 & 0 & 0 & 0 & 0 & 0 & 0 & 0 & 0 & 0 & 0 & 0 & 0 & 0 & 0 & 0\\
\frac{1}{R_1T_{sg1}} & 0 & -\frac{1}{T_{sg1}} & 0 & 0 & 0 & 0 & 0 & 0 & 0 & 0 & 0 & 0 & 0 & 0 & 0 & 0 & 0 & -\frac{k_{i1}}{T_{sg1}} & 0 & 0 & 0\\
0 & 0 & 0 & -\frac{1}{T_{ps2}} & \frac{K_{ps2}}{T_{ps2}} & 0 & 0 & 0 & 0 & 0 & 0 & 0 & \frac{a_{12}K_{ps2}}{T_{ps2}} & 0 & 0 & 0 & \frac{a_{32}K_{ps2}}{T_{ps2}} & \frac{a_{42}K_{ps2}}{T_{ps2}} & 0 & 0 & 0 & 0\\
0 & 0 & 0 & 0 & -\frac{1}{T_{t2}} & \frac{1}{T_{t2}} & 0 & 0 & 0 & 0 & 0 & 0 & 0 & 0 & 0 & 0 & 0 & 0 & 0 & 0 & 0 & 0\\
0 & 0 & 0 & -\frac{1}{R_2T_{sg2}} & 0 & -\frac{1}{T_{sg2}} & 0 & 0 & 0 & 0 & 0 & 0 & 0 & 0 & 0 & 0 & 0 & 0 & 0 & -\frac{k_{i2}}{T_{sg2}} & 0 & 0\\
0 & 0 & 0 & 0 & 0 & 0 & -\frac{1}{T_{ps3}} & \frac{K_{ps3}}{T_{ps3}} & 0 & 0 & 0 & 0 & 0 & -\frac{K_{ps3}}{T_{ps3}} & 0 & -\frac{K_{ps3}}{T_{ps3}} & -\frac{K_{ps3}}{T_{ps3}} & 0 & 0 & 0 & 0 & 0\\
0 & 0 & 0 & 0 & 0 & 0 & 0 & -\frac{1}{T_{t3}} & -\frac{1}{T_{t3}} & 0 & 0 & 0 & 0 & 0 & 0 & 0 & 0 & 0 & 0 & 0 & 0 & 0\\
0 & 0 & 0 & 0 & 0 & 0 & -\frac{1}{R_3T_{sg3}} & 0 & -\frac{1}{T_{sg3}} & 0 & 0 & 0 & 0 & 0 & 0 & 0 & 0 & 0 & 0 & -\frac{k_{i3}}{T_{sg3}} & 0 & \\
0 & 0 & 0 & 0 & 0 & 0 & 0 & 0 & 0 & -\frac{1}{T_{ps4}} & \frac{K_{ps4}}{T_{ps4}} & 0 & 0 & 0 & -\frac{K_{ps4}}{T_{ps4}} & \frac{a_{34}K_{ps4}}{T_{ps4}} & 0 & -\frac{K_{ps4}}{T_{ps4}} & 0 & 0 & 0 & 0\\
0 & 0 & 0 & 0 & 0 & 0 & 0 & 0 & 0 & 0 & -\frac{1}{T_{t4}} & \frac{1}{T_{t4}} & 0 & 0 & 0 & 0 & 0 & 0 & 0 & 0 & 0 & 0\\
0 & 0 & 0 & 0 & 0 & 0 & 0 & 0 & 0 & -\frac{1}{R_4T_{sg4}} & 0 & -\frac{1}{T_{sg4}} & 0 & 0 & 0 & 0 & 0 & 0 & 0 & 0 & 0 & -\frac{k_{i4}}{T_{sg4}}\\
2\pi T_{12} & 0 & 0 & -2\pi T_{12} & 0 & 0 & 0 & 0 & 0 & 0 & 0 & 0 & 0 & 0 & 0 & 0 & 0 & 0 & 0 & 0 & 0 & 0\\
-2\pi T_{31} & 0 & 0 & 0 & 0 & 0 & 2\pi T_{31} & 0 & 0 & 0 & 0 & 0 & 0 & 0 & 0 & 0 & 0 & 0 & 0 & 0 & 0 & 0\\
-2\pi T_{41} & 0 & 0 & 0 & 0 & 0 & 0 & 0 & 0 & 2\pi T_{41} & 0 & 0 & 0 & 0 & 0 & 0 & 0 & 0 & 0 & 0 & 0 & 0\\
0 & 0 & 0 & 0 & 0 & 0 & 2\pi T_{34} & 0 & 0 & -2\pi T_{34} & 0 & 0 & 0 & 0 & 0 & 0 & 0 & 0 & 0 & 0 & 0 & 0\\
0 & 0 & 0 & -2\pi T_{32} & 0 & 0 & 2\pi T_{32} & 0 & 0 & 0 & 0 & 0 & 0 & 0 & 0 & 0 & 0 & 0 & 0 & 0 & 0 & 0\\
0 & 0 & 0 & -2\pi T_{42} & 0 & 0 & 0 & 0 & 0 & 2\pi T_{42} & 0 & 0 & 0 & 0 & 0 & 0 & 0 & 0 & 0 & 0 & 0 & 0\\
b_1 & 0 & 0 & 0 & 0 & 0 & 0 & 0 & 0 & 0 & 0 & 0 & 1 & -a_{31} & -a_{41} & 0 & 0 & 0 & 0 & 0 & 0 & 0\\
0 & 0 & 0 & b_2 & 0 & 0 & 0 & 0 & 0 & 0 & 0 & 0 & -a_{12} & 0 & 0 & 0 & -a_{32} & -a_{42} & 0 & 0 & 0 & 0\\
0 & 0 & 0 & 0 & 0 & 0 & b_3 & 0 & 0 & 0 & 0 & 0 & 0 & 1 & 0 & 1 & 1 & 0 & 0 & 0 & 0 & 0\\
0 & 0 & 0 & 0 & 0 & 0 & 0 & 0 & 0 & b_4 & 0 & 0 & 0 & 0 & 1 & -a_{34} & 0 & 1 & 0 & 0 & 0 & 0
\end{bmatrix}$$

Considering Δf_1, Δf_2, Δf_3, and Δf_4 (*i.e.* change in frequency) and $\Delta P_{tie,\ 12}$ (change in tie line power) as system output variables, then output matrix will be the form of $y=Cx+Dw$ where, D=0, and C and X are given as:

$$C=\begin{bmatrix}
1 & 0 & 0 & 0 & 0 & 0 & 0 & 0 & 0 & 0 & 0 & 0 & 0 & 0 & 0 & 0 & 0 & 0 & 0 & 0 & 0 & 0\\
0 & 0 & 0 & 1 & 0 & 0 & 0 & 0 & 0 & 0 & 0 & 0 & 0 & 0 & 0 & 0 & 0 & 0 & 0 & 0 & 0 & 0\\
0 & 0 & 0 & 0 & 0 & 0 & 1 & 0 & 0 & 0 & 0 & 0 & 0 & 0 & 0 & 0 & 0 & 0 & 0 & 0 & 0 & 0\\
0 & 0 & 0 & 0 & 0 & 0 & 0 & 0 & 0 & 1 & 0 & 0 & 0 & 0 & 0 & 0 & 0 & 0 & 0 & 0 & 0 & 0\\
0 & 0 & 0 & 0 & 0 & 0 & 0 & 0 & 0 & 0 & 0 & 0 & 1 & 0 & 0 & 0 & 0 & 0 & 0 & 0 & 0 & 0
\end{bmatrix}$$

$$x^T=[x_1 \quad x_2 \quad x_3 \quad \bullet \quad \bullet \quad \bullet \quad x_{21} \quad x_{22}]$$

The control signal for the PI controller similarly can be given as:

$$u_i=-K_{pi}ACE_i-\int K_{ii}ACE_i\,dt \tag{5}$$

Where, K_{pi} and K_{ii} are respectively the proportional and integral gains of the PI controller.

The detailed block diagram modeling of four-area thermal power system under investigation is shown in Figure 3 for area 1. All areas comprise single reheat thermal system with governor dead band, generation rate constraint non-linearities and boiler dynamics. The list of symbols of the system is given in the Nomenclature and all the data used is given in Appendix.

Governor Deadband

The detailed transfer function models of the speed governors and turbines are discussed in [35], [41]. Governor deadband is defined as the total magnitude of a sustained speed change within which there is no resulting change in valve position. The Backlash non-linearity tends to produce continuous sinusoidal oscillations with a time period of about 2 seconds [35], [41]. The speed governor deadband has significant effect on the dynamic performance of load frequency control system. Describing function approach is used to incorporate the governor deadband non-linearity [41]. The hysteresis type of non-linearities is expressed as,

$$y=F(x,\dot{x}) \text{ rather than } y=F(x) \tag{6}$$

To solve the non-linear problem, it is necessary to make the basic assumption that the variable x, appearing in Equation 6 is sufficiently close to a sinusoidal Equation 7, that is,

$$x \approx A \sin w_0 t \tag{7}$$

Where, a is amplitude of oscillation and w_0 is frequency of oscillation.

$$w_0=2\pi f_0=\pi$$

As the variable function is complex and periodic function of time, it can be developed in a Fourier series [41] as:

$$F(x,\dot{x})=F^0+N_1x+\frac{N_2}{w_0}\dot{x}+\cdots \tag{8}$$

To solve this, it is a reasonable good to consider the first three terms only. The corresponding coefficients are:

$$F^0=\frac{1}{2\pi}\int_0^{2\pi}F(A\sin w_0t, A\,w_0\cos w_0t)\,d(w_0t)$$

$$N_1=\frac{1}{\pi A}\int_0^{2\pi}F(A\sin w_0t, A\,w_0\cos w_0t)\sin w_0t\,d(w_0t)$$

$$N_2=\frac{1}{\pi A}\int_0^{2\pi}F(A\sin w_0t, A\,w_0\cos w_0t)\cos w_0t\,d(w_0t) \tag{9}$$

As the backlash non-linearity is symmetrical about the origin, F^0 is zero. For the analysis in this paper, backlash is chosen 0.05% approximately [19]. The

Fourier coefficients are derived as: N_1=0.8 & N_2= -0.2. Thus Equation 8 can be written as follows:

$$F(x,\dot{x})=0.8x-\frac{0.2}{\pi}\dot{x}$$

Thus transfer function of the governor taking deadband into account, can be express as:

$$G_{sgi}(s)=\frac{N_1+N_2 s}{1+T_{sgi}s}$$

$$i.e.\quad G_{sgi}(s)=\frac{0.8-\frac{0.2}{\pi}s}{1+T_{sgi}s} \tag{10}$$

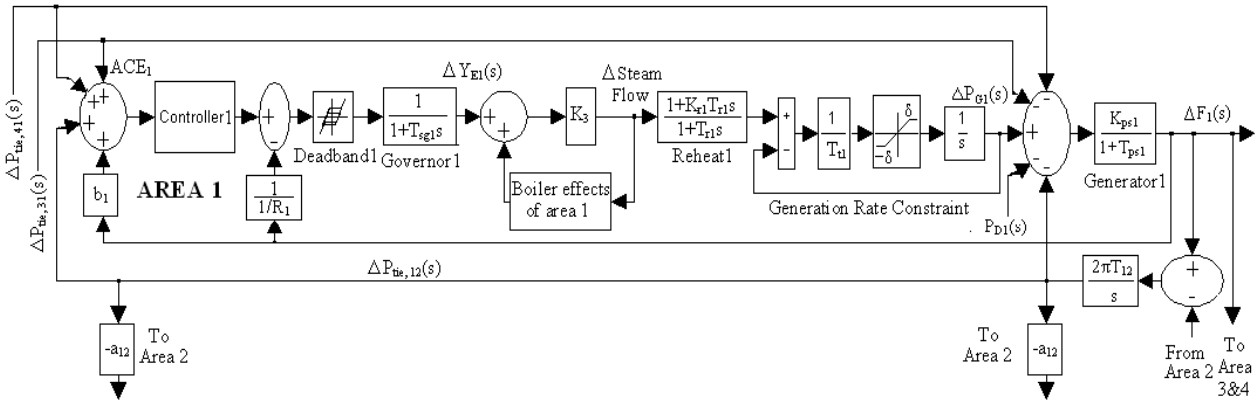

Fig. 3. Area 1 of four-area power system.

Generation Rate Constraint

In practical steam turbine systems, due to thermo-dynamic and mechanical constraints, there is a limit to the rate at which its output power ($\Delta \dot{P}_g$) can be changed. This limit is referred as generation rate constraint (GRC). It is obvious that the dynamic responses of the system with the presence of GRC have larger overshoots and longer settling times, compared to the system without GRC. For all the four thermal areas a generating rate limitation of 10% per minute is considered [39].

$$i.e.\ \Delta \dot{P}_g \le 0.1\ \text{puMW/Min.}=0.0017\ \text{puMW/s}=\delta$$

The GRC is taken into account by adding a limiter (δ= ±0.0017) to the turbine power.

Boiler Dynamics

The changes in generation are initiated by turbine control valves. Changes in steam flow and pressure are sensed and thus control the combustion rate. Boiler is a device meant for producing steam under pressure. The model shown in Figure 4 explained in details in [42]-[43] is basically for a drum type boiler. This includes the long term dynamics of fuel and steam flow on boiler drum pressure. Representations for combustion controls are also incorporated. Even though the model is basically for a drum type boiler, similar responses have been observed for once- through boilers and pressurized water reactors [42]. The boiler receives feed water which has been preheated in the economizer and provides saturated steam outflow. Recirculation boiler makes use of a drum to separate steam flow from the recirculation water so that it can proceed to the super heater as a heatable vapour. The changes in generations are initiated by turbine control valves and the boiler controls respond with necessary control action, change in steam flow and change in throttle pressure, the combustion rate and hence the boiler output. The model can be used to study the responses of coal fired units with poorly tuned (oscillatory) combustion controls, coal fired units with well-tuned controls and well-tuned oil or gas fired units.

3. FUZZY LOGIC BASED PI CONTROLLER

Fuzzy logic (FL) control is based on a logical system called fuzzy logic which is much closer in spirit to human thinking and natural language than classical logical systems. In recent years, FL has emerged as a complement tool to mathematical approaches for solving power system problems. Fuzzy set theory and fuzzy logic establish the rules of a non-linear mapping. These rules are obtained based on experiments of the process step response, error signal, and its time derivative [39]. The FLPI controller (Figure 5) to solve the four-area LFC problem (Figure 2) consists of a FL controller and a conventional PI controller, connected in series. The FL controller has two input signals, namely, ACE and derivative of ACE, and then the output signal (y) of the fuzzy logic controller is the input signal of the conventional PI controller. Finally, the output signal from the conventional PI controller called the control signal (u) is used for controlling the LFC in the interconnected power system.

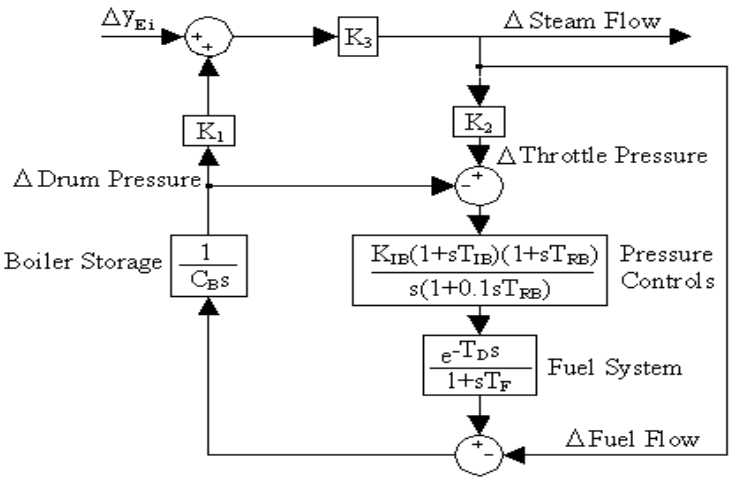

Fig. 4. Block diagram of boiler dynamics [34]-[40].

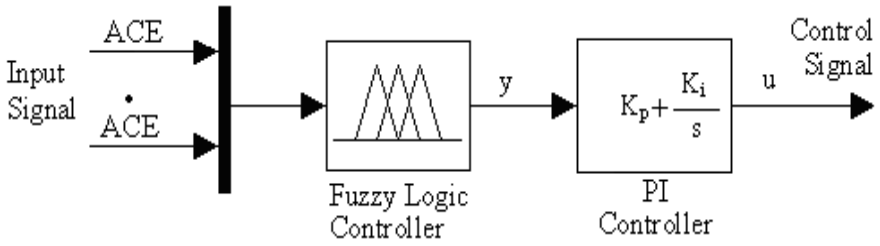

Fig. 5. Structure of fuzzy logic based proportional integral controller.

The fuzzy controller is comprised of four main components [44]: the fuzzification, the inference engine, the rule base, and the defuzzification, as shown in Figure 6. The fuzzifier transforms the numeric/crisp value into fuzzy sets, so that, this operation is called fuzzification. The main component of the fuzzy logic controller is the inference engine, which performs all logic manipulations in a fuzzy logic controller. The rule base consists of membership functions and control rules. Last, the results of the inference process is an output represented by a fuzzy set, however, the output of the fuzzy logic controller should be a numeric/crisp value. Therefore, fuzzy set is transformed into a numeric value by using the defuzzifier, so that, this operation is called defuzzification. The control signal is given by

$$u_i(t) = -(K_{pi} y + \int K_{ii} y dt) \quad (11)$$

K_{pi} and K_{ii} are the proportional and the integral gains respectively. For the proposed study Mamdani fuzzy inference engine was selected and the centroid method is used in defuzzification process.

Fuzzy logic shows experience and preference through membership functions. These functions have different shapes depending on system experts' experience [23]. The membership functions of the fuzzy logic controller for inputs and output presented in Figure 7 consist of three memberships functions (two-inputs and one-output). Each membership function has seven memberships, comprising two trapezoidal and five triangular memberships. The number of rules in inference mechanism is taken seven. Therefore, 49 control rules are used for this study. The ranges of the membership functions are chosen from simulation results. The control rules build from the if-then statement (if input 1 and input 2 then output 1). Table 1 indicates the appropriate rule base [28], [44]. For example the third row and third column in Table 1 indicates if ACE is SN and d derivative of ACE is SN then *y* is SP.

4. RESULTS AND DISCUSSION

Simulations were performed using the conventional PI controller and the proposed fuzzy logic based PI controllers applied to a four-area interconnected electrical power system with 0.01 and 0.02 puMW step load disturbances in area1. The same system data given in Appendix is used in both controllers to make a comparison. The implementations were carried out with MATLAB7.5/SIMULINK software. The simulations were run on a personal computer Intel Core2Duo CPU T5450 @ 1.66 GH_Z, 982 MH_Z, 2GB of RAM, under Window XP.

For the conventional PI (also PI of FLPI) controller, the gains of proportional and integral are chosen 0.01 and 0.04, respectively. These optimum values are determined experimentally for conventional PI controller.

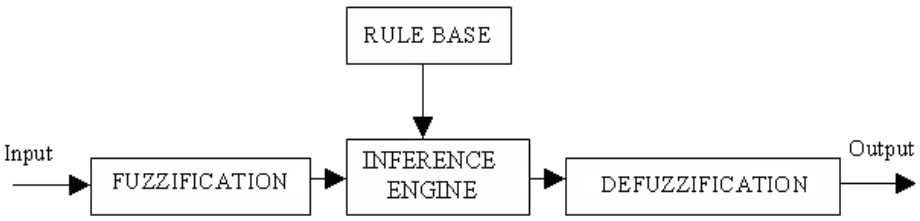

Fig. 6. Components of a fuzzy logic controller.

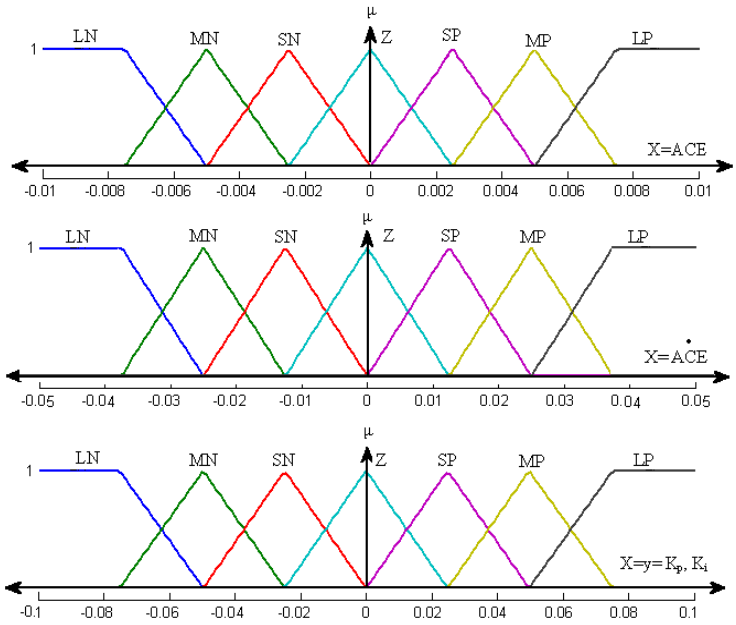

Fig. 7. Membership functions of fuzzy controller.

Table 1. Control rules for FLPI controller.

	$\dot{A}CE$							
		LN	MN	SN	Z	SP	MP	LP
	LN	LP	LP	LP	MP	MP	SP	Z
	MN	LP	MP	MP	MP	SP	Z	SN
A	SN	LP	MP	SP	SP	Z	SN	MN
C	Z	MP	MP	SP	Z	SN	MN	MN
E	SP	MP	SP	Z	SN	SN	MN	LN
	MP	SP	Z	SN	MN	MN	MN	LN
	LP	Z	SN	MN	MN	LN	LN	LN

LN: Large Negative, MN: Medium Negative, SN: Small Negative, Z: Zero, SP: Small Positive, MP: Medium Positive, LP: Large Positive

Four-Area System with Equal Power Ratings

The dynamic response of four-area system containing all areas of equal power ratings for 1% load disturbance in area 1 is shown in Figures 8 and 9. The FLPI controller is significantly superior to the conventional PI controller. It gives a better dynamic performance than PI controller. The settling time and peak overshoots are reduced considerably. The simulation results of frequency deviations and tie line power deviation with FLPI controller advocates its suitability for LFC schemes, which is also verified through proper settlement of area control error. The area control error is defined as a quantity reflecting the deficiency or excess of power within a control area. Here, ACE of all four areas is also effectively controlled with the proposed controller.

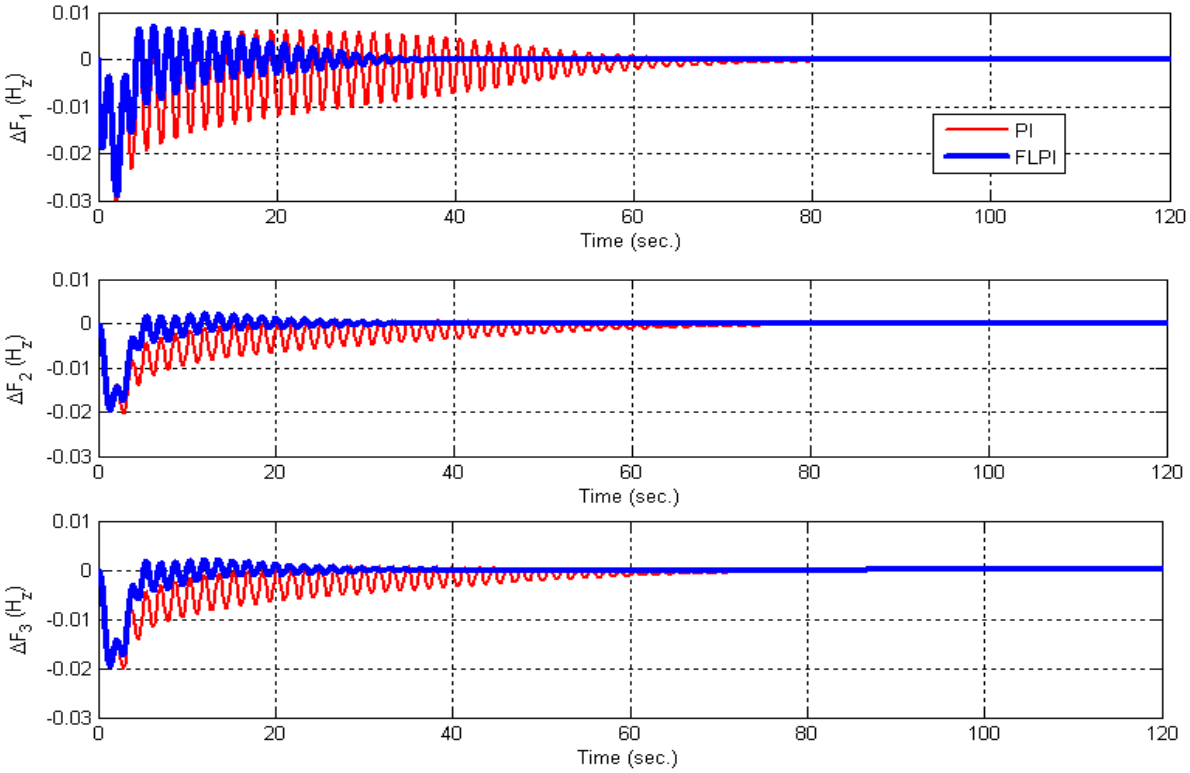

(a)

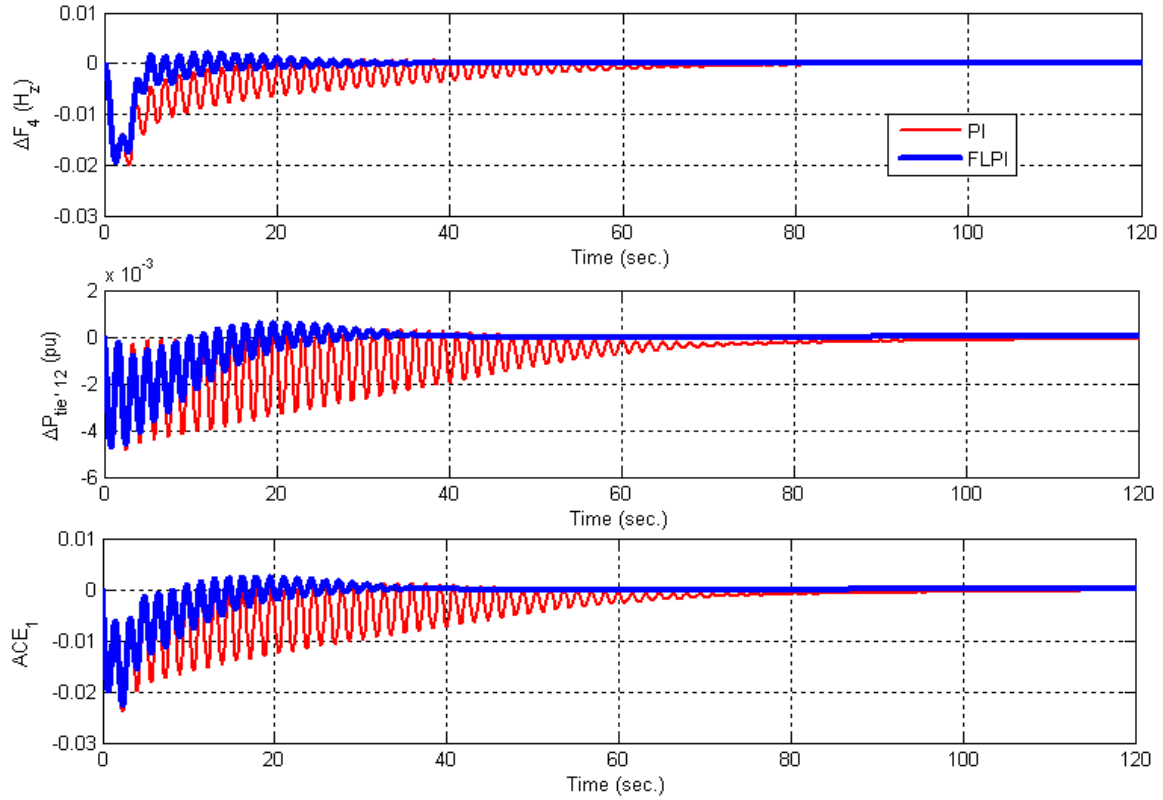

(b)

Fig. 8. Deviation in frequency of (a) area 1-3 (b) area 4, change in tie line power ($\Delta P_{tie,12}$), and area 1 area control error (ACE_1) at ΔP_{d1} =0.01 pu.

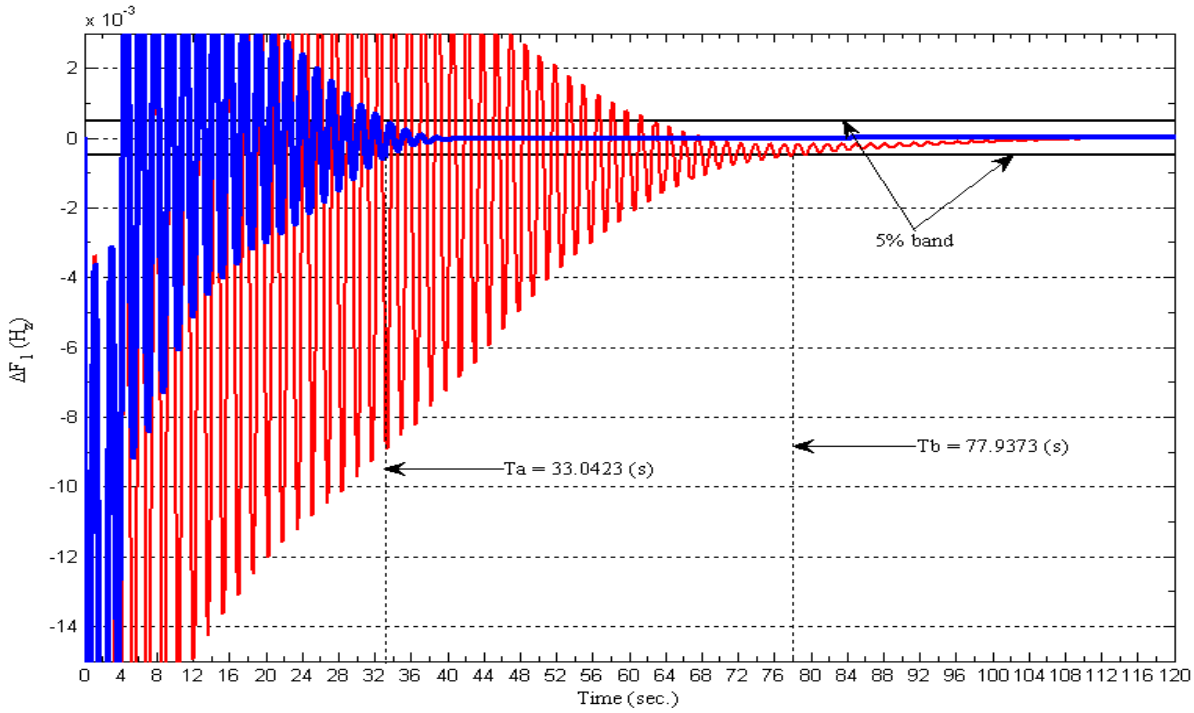

Fig. 9. Deviation of frequency of area 1 in a large scale and settling times for proposed FLPI controller (Ta) and PI controller (Tb) at ΔP_{d1} =0.01 pu.

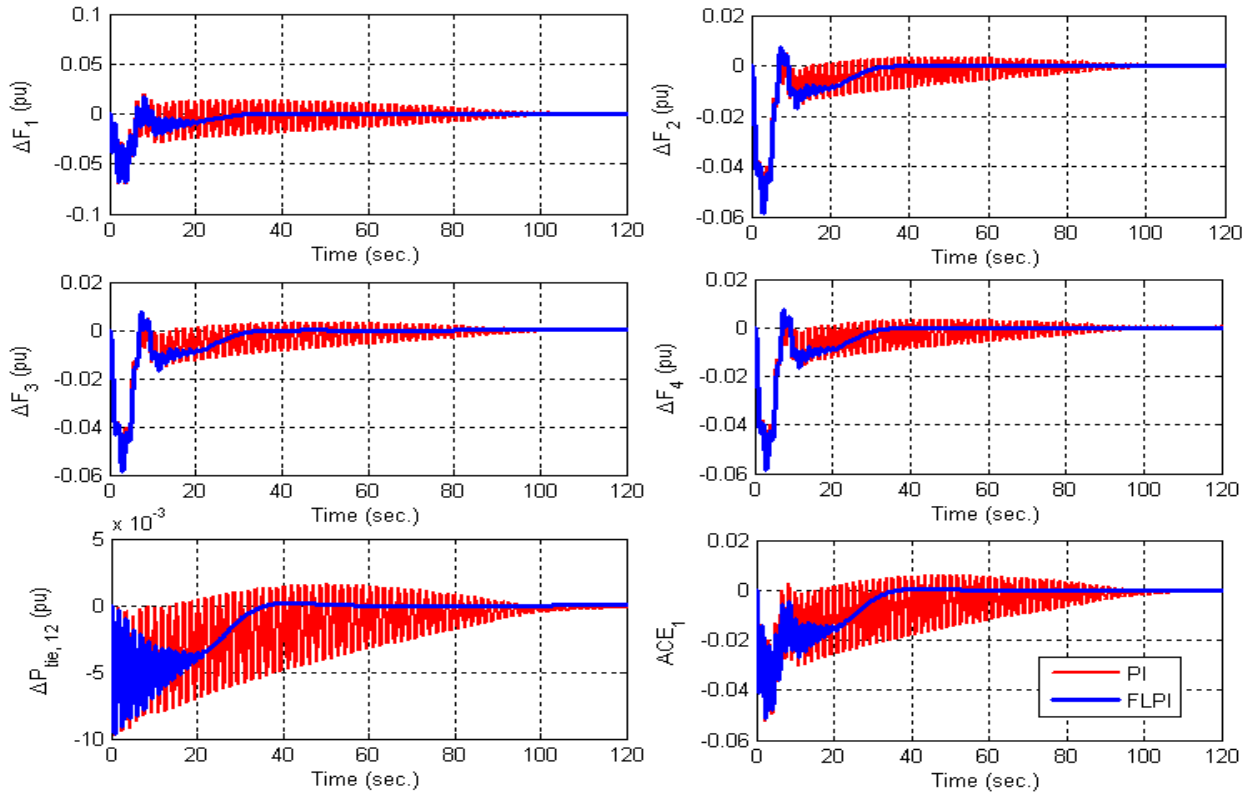

Fig. 10. Deviation in frequency of area 1-4, change in tie line power ($\Delta P_{tie,12}$), and area 1 area control error (ACE_1) at ΔP_{d1} =0.02 pu.

The frequency deviation of area 1 with settling time for 5% band of the step load change and maximum overshoots are given in Table 2. The comparison of dynamic performances of the proposed controller with other controllers indicates better response of FLPI in terms of lesser settling time and peak overshoot.

The simulation results show that proposed controller for load frequency control is giving approximately 22.25% reduction in settling time and 40.49% reduction in peak overshoots when compared with B. Anand's study (for two-area with same values of parameters).

Also a reduction of 3.35% and 57.6% respectively in settling time and peak overshoot observed while comparing performance of FLPI and PI controllers.

The dynamic response of four-area system containing all areas of equal power ratings for 2% load disturbance in area 1 is shown in Figure 10. The responses of the controllers given in Table 3 and shown in Figure 10, also confirm that the FLPI can effectively stabilize frequency oscillations under different load disturbance conditions.

In the analysis of the simulation results, the frequency deviation results were also used to calculate the integral absolute error (IAE) and integral of time multiplied absolute error (ITAE) of area 1 for both controllers as given in Equations 12 and 13 for 120 seconds of simulation time.

$$IAE=\int_0^{120}|\Delta f_1|dt \tag{12}$$

$$ITAE=\int_0^{120} t\,|\Delta f_1|dt \tag{13}$$

The values of IAE and ITAE are calculated at 1% load disturbance in area 1. System performance of the controllers given in Table 4 shows that proposed FLPI controller has less IAE and ITAE as compared to conventional PI controller for four-area power system equipped with all areas of equal ratings.

Table 2. Dynamic performance of the controllers.

Deviation in frequency (Δf_1)	Settling time (sec.) for 5% band	Peak overshoot (pu)
FLPI Controller (Ta)	33.0423	-0.0288
B. Anand's study for two-area system [39]	42.5	-0.0484
PI Controller (Tb)	77.9373	-0.0298

Table 3. Dynamic performance of the controllers.

Deviation in frequency(Δf_1)	Settling time (sec.) for 5% band	Peak overshoot (pu)
FLPI Controller	31.8354	-0.0687
PI Controller	109.004	-0.0696

Table 4. Performance in terms of IAE and ITAE.

Controllers	IAE	ITAE	IAE	ITAE
	ΔP_{d1}=0.01 (pu)		ΔP_{d1}=0.02 (pu)	
FLPI Controller	0.1292	1.193	0.4208	3.85
PI Controller	0.3438	7.953	1.003	32.89

Table 5. Performance in terms of IAE and ITAE.

Controllers	IAE	ITAE	IAE	ITAE
	ΔP_{d1}=0.01 (pu)		ΔP_{d1}=0.02 (pu)	
FLPI Controller	0.1574	2.98	0.1641	1.499
PI Controller	1.84	128.2	2.055	133.2

Four-Area System with Unequal Power Ratings

Other simulations are carried out on interconnected four-area power system, with power ratings of area 1: 2000 MW, area 2: 4000MW, area 3: 6000MW, and area 4: 8000 MW. The comparison of dynamic performance of two controllers with disturbance of 1% in area 1 (ΔP_{d1} =0.01 pu) is shown in Figure 11 and with disturbance of 2% in area 1 (ΔP_{d1} =0.02 pu) is shown in Figure 12. For simulation time of 120 seconds, the values of IAE and ITAE for deviation of frequency in area 1 (Δf_1) with disturbance of 1% and 2% in area 1 are given in Table 5.

From Figures 11 and 12, and Table 5, it is concluded that FLPI controller when compared with conventional PI controller, provide better dynamic response in terms of lesser settling time, peak overshoot, oscillations, IAE, and ITAE. Hence performance of FLPI controller is best whether four-area power system is equipped with equal power rating units or unequal power rating units. This also confirms the robustness of the FLPI controller which works well at different types of systems.

Simulations are also carried out for ±35% change in parameter values (mainly b_i, T_{ij} and $T_{psi.}$) of the system containing equal power rating areas. Parameters are changed in all four areas at the same time. In Figure 13, the responses are shown with +35% change in system parameter values at 1% load change in area 1. It indicates that change in frequency (areas 1-4), change in tie-line power $\Delta P_{tie,\,12}$, and area control error (ACE_1), are getting settled down within reasonably good time. Similarly with same amount of disturbance in area 1, it is observed that the system is settled down quite fast with -35% changes in system parameter values as indicated in Figure 14. This justifies the robustness of the proposed controller, which is capable to withstand the changes in dynamic parameters of the system.

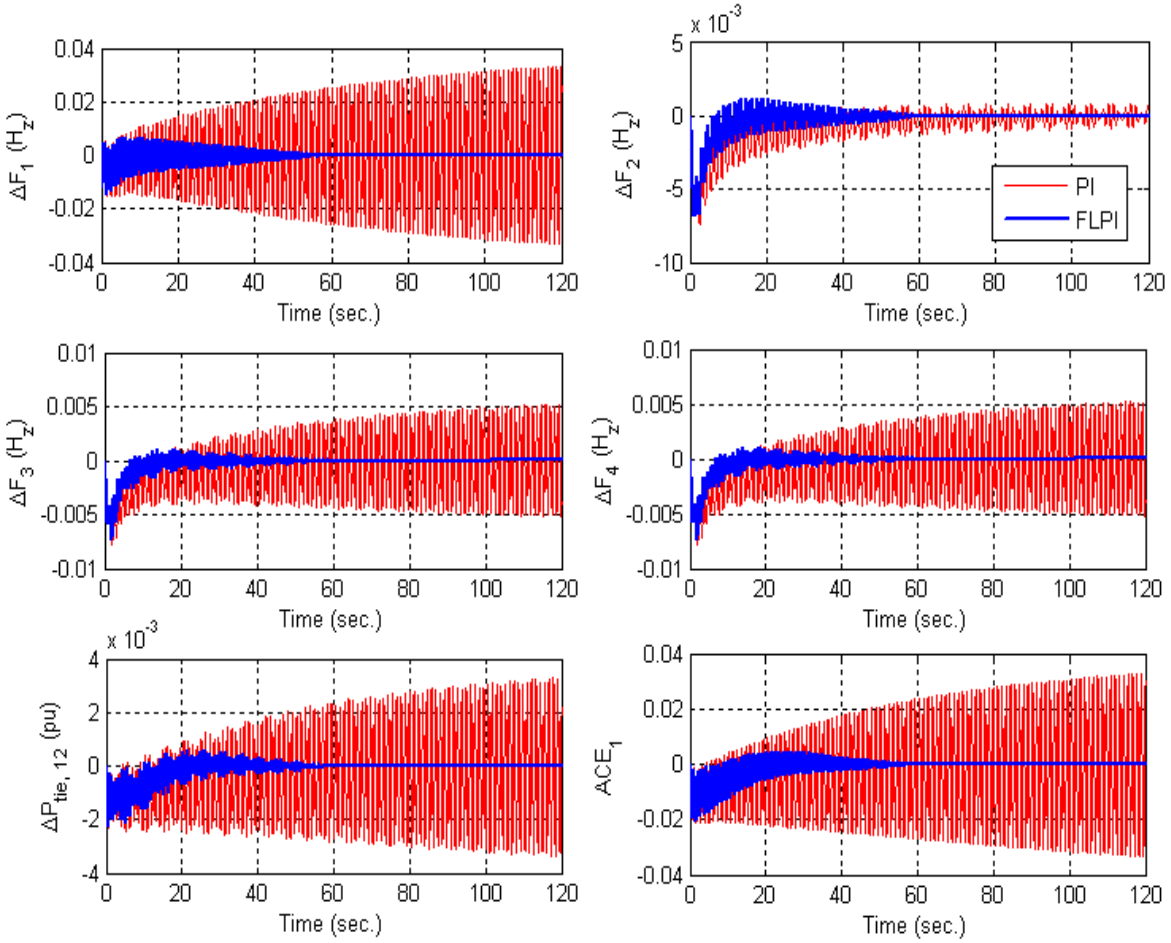

Fig. 11. For unequal power system, deviation in frequency of area 1-4, $\Delta P_{tie,12}$, and ACE_1 at ΔP_{d1} =0.01 pu.

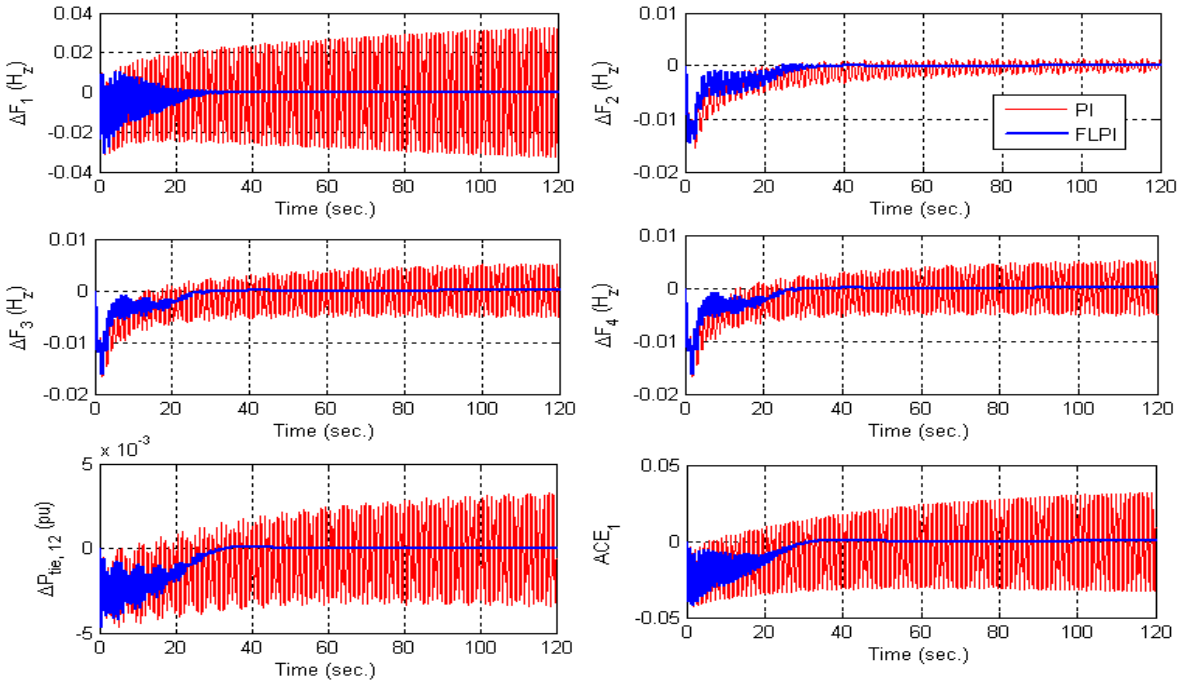

Fig. 12. For unequal power system, deviation in frequency of area 1-4, $\Delta P_{tie,12}$, and ACE_1 at ΔP_{d1} =0.02 pu.

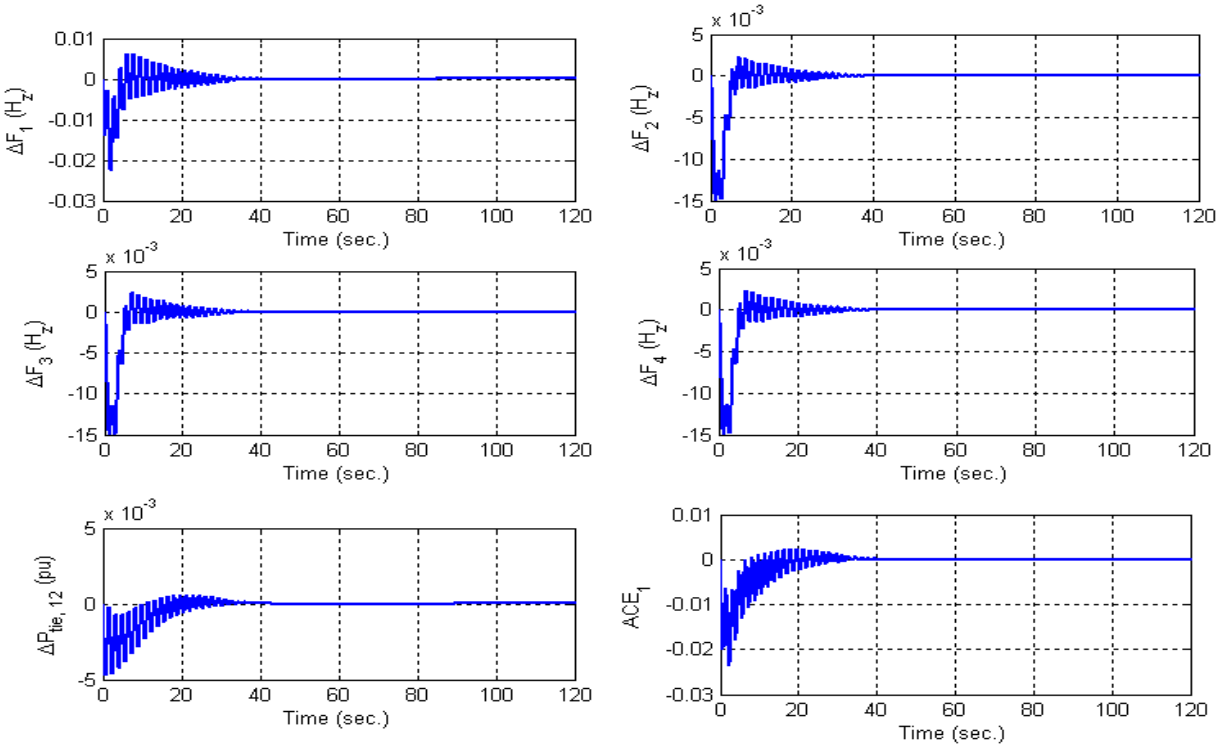

Fig. 13. Deviation in frequency of area 1-4, $\Delta P_{tie,12}$, and ACE_1 at ΔP_{d1} =0.01 pu with FLPI controller at +35% change in parameters of equal area power system.

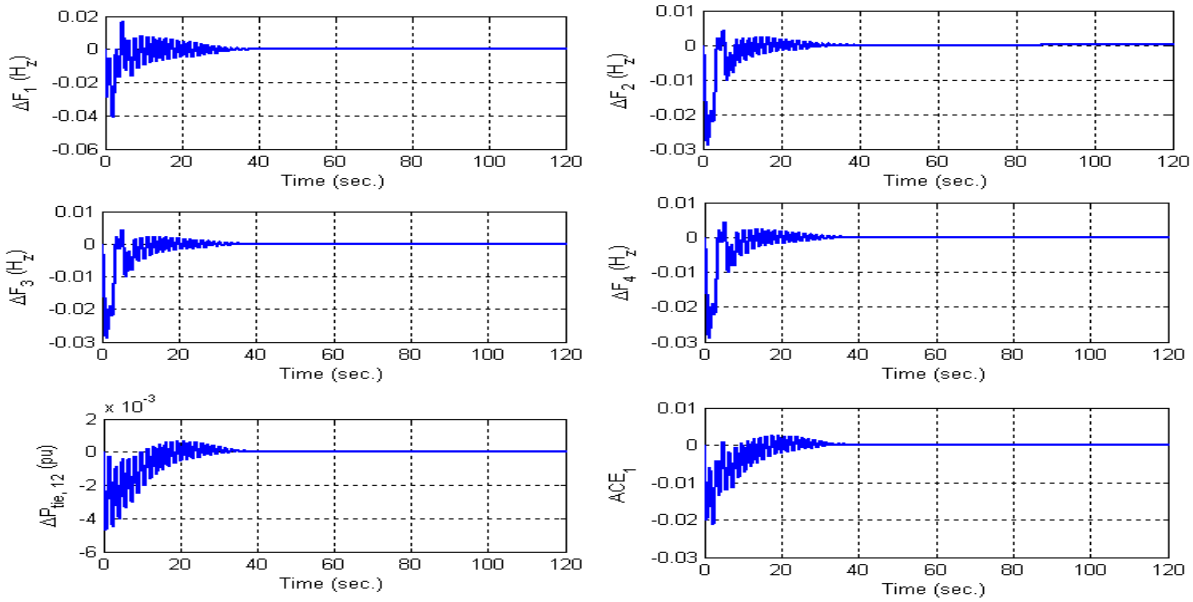

Fig. 14. Deviation in frequency of area 1-4, $\Delta P_{tie,12}$, and ACE_1 at ΔP_{d1} =0.01 pu with FLPI controller at -35% change in parameters of equal area power system.

5. CONCLUSION

In this paper, a fuzzy logic based PI (FLPI) controller is designed for automatic load frequency control in four-area electrical power system. The performance of the controller is observed on the basis of four parameters *i.e.* settling time, peak overshoot, integral absolute error and integral of time multiplied absolute error. From the results it is concluded that the proposed FLPI controller provides better dynamic performance when compared with conventional PI controller applied to four-area power system considering single reheat thermal turbines with generation rate constraint, governor deadband and boiler dynamics. Robustness of the FLPI controller is also checked with changing the system and parameters of the system under study. In addition, the proposed controller is very simple and easy to implement.

NOMENCLATURE

Δf_i	incremental frequency deviation of i^{th} area, H_Z pu.
ΔP_{di}	incremental load demand change of i^{th} area, puMW.
T_{sgi}	speed governor time constant of i^{th} area, sec.
K_{sgi}	gain of speed governor of i^{th} area.
R_i	governor speed regulation of i^{th} area, H_Z/puMW.
T_{ti}	turbine time constant of i^{th} area, sec.
K_{psi}	gain of power system of i^{th} area, H_Z /puMW.
T_{psi}	power system time constant of i^{th} area, sec.
ΔP_{gi}	incremental generator/turbine power output change of i^{th} area, puMW.
ΔP_{ci}	incremental speed changer setting change of i^{th} area, puMW.
Δy_{Ei}	incremental steam valve setting change of i^{th} area, puMW.
K_{ii}	gain of integral controller of i^{th} area.
b_i	frequency bias of i^{th} area, puMW/H_Z.
ACE_i	area control error of i^{th} area, puMW.
u_i	control input of i^{th} area.
w_i	disturbance vector of i^{th} area, puMW.
$\Delta P_{tie,ij}$	incremental tie line power change of i^{th} and jth area, puMW.
a_{ij}	area size ratio coefficient (=P_{ri}/P_{rj})
P_{ri}	rated power of i^{th} area.
P_{rj}	rated power of j^{th} area.
T_{ij}	tie line synchronizing power co-efficient (pu) between area i and area j.
K_{ri}	transfer function gains of reheats of i^{th} area
T_{ri}	reheat time constant of i^{th} area turbine, sec.
w_0	angular frequency of natural sinusoidal oscillation
N_1	Fourier series coefficient associated with x
N_2	Fourier series coefficient associated with sx
k	slope of input/output curve of governor
T_D	fuel firing system delay time, sec.
T_F	fuel system time constant, sec.
C_B	boiler storage time constant, sec.
T_{RB}	lead-lag compensator time, (sec).
K_{IB}	boiler integrator gain
T_{IB}	proportional-integral ratio of gains

REFERENCES

[1] Elgerd O.I., 2008. *Electric Energy Systems Theory: An Introduction*. 2nd ed. 30th reprint. New Delhi: Tata McGraw-Hill.

[2] Fosha C.E. and O.I. Elgerd. 1970. The megawatt-frequency control problem: a new approach via optimal control theory. *IEEE Transactions on Power Appratus and Systems* 89(4):563-577.

[3] Gupta S.K., 2009. *Power System Engineering*. 1st ed. New Delhi: Umesh Publishers.

[4] Saadat H., 2002. *Power System Analysis*, 1st ed. 15th reprint. New Delhi: Tata McGraw Hill Publishing Company Limited.

[5] Arya Y., Kumar N. and Gupta S.K., 2012. Load frequency control of a four-area power system using linear quadratic regulator. *International Journal of Energy Science* 2(2):69-76.

[6] Malik O.P., Hope G.S., Tripathy S.C. and Mital N., 1985. Decentralized suboptimal load-frequency Control of a hydro-thermal power system using the state variable model. *Electrical Power Systems Research* 8(3):237-247.

[7] Ibraheem, Kumar P., Hasan N. and Nizamuddin. 2012. Sub-optimal automatic generation control of interconnected power system using output vector feedback control strategy. *Electrical Power Components and Systems* 40(9):977-994.

[8] Hasan N., Ibraheem, Kumar P. and Nizamuddin. 2012. Sub-optimal automatic generation control of interconnected power system using constrained feedback control strategy. *Electrical Power and Energy Systems* 43(1):295-303.

[9] Malik O.P., Kumar A. and Hope G.S., 1988. A load frequency control algorithm based on generalized approach. *IEEE Transactions on Power Systems* 3(2):375-382.

[10] Das D., Nanda J., Kothari M.L. and Kothari D.P., 1990. Automatic generation control of a hydrothermal system with new area control error considering generation rate constraint. *Electric Machines and Power Systems* 18(6):461-471.

[11] Shoults R.R. and J.A.J. Ibarra. 1993. Multi-area adaptive LFC developed for a comprehensive agc simulator. *IEEE Transactions on Power Systems* 8(2):541-547.

[12] Rubaai, A. and V. Udo. 1994. Self-tuning load frequency control: multilevel adaptive approach. *IEE Proceedings on Generation Transmission Distribution* 141(4):285-290.

[13] Olmos L., de la Fuente J.I., Macho J.L.Z., Pecharroman R.R., Calmarza A.M. and Moreno J., 2004. New design for the Spanish agc scheme using an adaptive gain controller. *IEEE Transactions on Power Systems* 19(3):1528-1537.

[14] Kothari M.L., Das D, Singh S.V., Kothari D.P. and Nanda J., 1991. Variable structure controllers for agc of interconnected power system. *Journal of Institution of Engineers India* 72(EL):79-82.

[15] Das D., Kothari M.L., Kothari D.P. and Nanda J., 1991. Variable structure control strategy to automatic generation control of interconnected reheat thermal system. *IEE Proceeding-D Control Theory and Applications* 138(6):579-585.

[16] Al-Hamouz Z.M. and Y.L. Abdel-Magid. 1993. Variable-structure load frequency controllers for multiarea power systems. *Electrical Power and Energy Systems* 15(5):293-300.

[17] Doolla S., Bhatti T.S. and Bansal R.C., 2010. Variable structure load frequency control of an isolated small hydro power plant. *International Journal of Electrical Energy Systems* 2(1):19-26.

[18] Chaturvedi D.K., Satsangi P.S. and Kalra P.K., 1999. Load frequency control: a generalized neural network approach. *Electrical Power and Energy Systems* 21(6):405-415.

[19] Oysal Y., 2005. A comparative study of adaptive load frequency controller design in a power system with dynamic neural network models. *Energy Conversion and Management* 46(15):2656-2668.

[20] Luy M., Kocaarslan I., Cam E. and Taplamacioglu, M.C., 2008. Load frequency in single area power system by artificial neural network. *University of Pitesti Electronics and Computers Science Scientific Bulletin* 8(2):26-29.

[21] Saikia L.C., Mishra S., Sinha N. and Nanda J., 2011. Automatic generation control of a multi area hydrothermal system using reinforced learning neural network controller. *Electrical Power and Energy Systems* 33(4):1101-1108.

[22] Ogbonna B. and S.N. Ndubisi. 2012. Neural network based load frequency control for restructuring power industry. *Nigerian Journal of Technology* 31(1):40-47.

[23] Cam E. and I. Kocaarslan. 2005. A fuzzy gain scheduling pi controller application for an interconnected electrical power system. *Electrical Power Systems Research* 73(3):267-274.

[24] Cam E. and I. Kocaarslan. 2005. Load frequency control in two area power system using fuzzy logic controller. *Energy Conversion and Management*, 46(2):233-243.

[25] Mathur H.D. and H.V. Manjunath. 2006. Extended fuzzy logic based integral controller for three area power system with generation rate constraint. *IEEE International Conference on Industrial Technology*, Mumbai, India, 15-17 December, 917-921.

[26] Sreenath A., Atre Y.R. and Patil D.R., 2008. Two area load frequency control with fuzzy gain scheduling of pi controller. *IEEE Computer Society 1st International Conference on Emerging Trends in Engineering and Technology*, Nagpur, Maharashtra, 16-18 July, 899-904.

[27] Suhag S. and A. Swarup. 2011. Automatic generation control of multi-area multi unit power system with SMES using fuzzy gain scheduling approach. *International Journal of Research and Reviews in Electrical and Computer Engineering*, 1(2):83-91.

[28] Arya Y., Mathur H.D. and Gupta S.K., 2012. A novel approach for load frequency control of interconnected thermal power stations. *International Journal of Energy Optimization and Engineering* 1(2):85-95.

[29] Panda G., Panda S. and Ardil C., 2009. Automatic generation control of interconnected power system with generation rate constraints by hybrid neuro fuzzy approach. *International Journal of Electrical Power and Energy Systems Engineering* 2(1):13-18.

[30] Dhanalakshmi R. and S. Palaniswami. 2012. ANFIS based neuro-fuzzy controller in lfc of wind-micro hydro-diesel hybrid power system. *International Journal of Computer Applications* 42(6):28-35.

[31] Ibraheem, Singh O. and Hasan N., 2010. Genetic algorithm based scheme for optimization of agc gains of interconnected power system. *Journal of Theoretical and Applied Information Technology* 12(1):33-39.

[32] Golpira H., Bevrani H. and Golpira H., 2011. Application of ga optimization for automatic generation control design in an interconnected power system. *Energy Conversion and Management* 52(5):2247-2255.

[33] Vijay M. and D. Jena. 2012. A continuous-discrete mode of optimal control of agc for multi area hydrothermal system using genetic algorithm. *Proceedings of IEEE International Conference Computing, Communication and Applications*, Dindigul, Tamilnadu, 22-24 Febebruary, 1-6.

[34] Tripathy S.C., Balasubramanian R. and Nair P.S.C., 1991. Small rating capacitive energy storage for dynamic performance improvement of automatic generation control. *IEE Proc.-C Generation Transmission Distribution* 138(1):103-111.

[35] Tripathi S.C., Balasubramanian R. and Nair P.S.C., 1992. Effect of superconducting magnetic energy storage on automatic generation control considering governor deadband and boiler dynamics. *IEEE Transactions on Power Systems* 7(3):1266-1273.

[36] Devotta J.B.X., Rabbani M.G. and Elangovan S., 1998. Effect of smes unit on agc dynamics. In *Proceedings of International Conference on Energy Management and Power Delivery*, Singapore, 3-5 March, 1: 61-66.

[37] Ngamroo I., 2005. An optimization technique of robust load frequency stabilizer for superconducting magnetic energy storage. *Energy Conversion and Management* 46(18-19):3060-3090.

[38] Pothiya S. and I. Ngamroo. 2008. Optimal fuzzy logic-based pid controller for load-frequency control including superconducting magnetic energy storage units. *Energy Conversion and Management* 49(10):2833-2838.

[39] Anand B. and A.E. Jeyakumar. 2009. Load frequency control with fuzzy logic controller considering non-linearities and boiler dynamics. *ICGST-ACSE Journal* 8(3):15-20.

[40] Ngamroo I., 2005. Robust decentralized frequency stabilizers design for smes taking into consideration system uncertainties. *Electrical Power Systems Research* 74(2):281-292.

[41] Tripathy S.C., Hope G.S. and Malik O.P., 1982. Optimisation of load-frequency control parameters for power systems with reheat steam turbines and governor deadband nonlinearity. *IEE Proc.-C Generation Transmission Distribution* 129(1):10-16.

[42] de Mello F.P., Mills R.J. and B'Rells W.F., 1973. Automatic generation control part I-Process modeling. *IEEE Transactions on Power Apparatus and systems* PAS-92(2):710-715.

[43] Shahrodi E.B. and A. Norched. 1985. Dynamic behavior of agc systems including the effects of nonlinearities. *IEEE Transactions on Power Appratus and Systems* PAS-104(12):3409-3415.

[44] Saikia L.C. and N. Sinha. 2010. Maiden application of fuzzy logic based IDD controller for automatic generation control of multi-area hydrothermal system: a preliminary study. *IEEE 20th Australasian University Power Engineering Conference*, Christchurch, New Zealand, 5-8, December, 1-6.

APPENDIX

Nominal parameters

(a) System data:

Nominal parameters of the four-area thermal power system investigated [23], [39]:

For thermal system with equal power units:
$P_{r1}= P_{r2}= P_{r3}=P_{r4}=2000$MW
For thermal system with unequal power units:
$P_{r1}=2000$MW, $P_{r2}=4000$MW, $P_{r3}=6000$MW, $P_{r4}=8000$MW

$R_1=R_2=R_3=R_4=2.4$ H_Z/puMW
$T_{sg1}=T_{sg2}= T_{sg3}= T_{sg4}=0.08$ seconds
$T_{t1}=T_{t2}= T_{t3}= T_{t4}=0.3$ seconds
$T_{ps1}=T_{ps2}=T_{ps3}=T_{ps4}=20$ seconds
$K_{ps1}= K_{ps2}=K_{ps3}=K_{ps4}=120$ H_Z/puMW
$T_{12}=T_{32}=T_{31}=T_{34}=T_{41}=T_{42}=0.08674$ puMW/Radian
$T_{r1} =T_{r2}= T_{r3}=T_{r4}=10$ seconds
$K_{r1}=K_{r2}= K_{r3}= K_{r4}=0.5$
$P_{tie,\ 12}= P_{tie,\ 32}= P_{tie,\ 31}= P_{tie,\ 34}= P_{tie,\ 41}= P_{tie,\ 42(max)} =200$ MW
F=60 H_Z
$a_{12}=a_{32}=a_{31}=a_{34}=a_{41}=a_{42}=1$
$\Delta P_{d1}=0.01$ puMW & $\Delta P_{d1}=0.02$ puMW
$\delta= \pm 0.0017$ puMW/s

(b) Boiler (gas or oil fired type) data [34]-[40]:

$K_1= 0.85$, $K_2= 0.095$, $K_3= 0.92$, $C_B=200$, $T_D= 0$, $T_F= 10$, $K_{IB}= 0.03$, $T_{IB}= 26$, $T_{RB}= 69$